

# Study of Stability Variations in Reaction Torque Observer based Force Controllers

W. M. Theekshana G. Wijewardhana  
Department of Electrical Engineering  
University of Moratuwa  
Katubedda, Sri Lanka  
theekshana.g.wijewardhana@gmail.com

A. M. Harsha S. Abeykoon  
Department of Electrical Engineering  
University of Moratuwa  
Katubedda, Sri Lanka  
harsha@uom.lk

**Abstract**—An effective method for determining the environmental impedance is to use a reaction torque observer (RTOB), which is a variant of the disturbance observer (DOB) concept. A robust yet accurate force controller can be developed by implementing both RTOB and DOB. This study examines the potential instability of force controllers based on RTOB. Traditionally, a RTOB-based force controller is examined under the presumption that the two cut-off frequencies for DOB and RTOB should always be equal to one another. But in some circumstances, it fails to maintain stability. The stability of the system is determined by the interactions between the mechanical, environmental, and controller dynamics, which also add to design constraints. There has not been any analysis of unstable scenarios in terms of system dynamics. In this paper, a novel stability constraint is derived as a result of the new stability assessment approach that is proposed. A new stability guideline is also suggested. The simulation results are used to confirm the validity of the proposals.

**Index Terms**—Disturbance observer (DOB), reaction torque observer (RTOB), force controller, motion control systems and stability.

## I. INTRODUCTION

DC motors are widely used in motion control systems such as position controllers, velocity controllers, and force controllers. Due to the limitations of conventional force measuring transducers, force controllers are the least popular of these control topologies [1]. The force sensor, as an example, can only sense force in the location to which it is attached [2]. They have a limited range of force sensing [1], [2]. Traditional force sensors can change system characteristics like mass and inertia when attached [3]. As a result, system dynamics and system transfer function may be affected. Robustness and accuracy are the desired properties of a motion control system [4], [5]. However, they are bounded by sensor limitations. Due to these disadvantages, force controllers are not very common in the context of control engineering.

A key component of motion control system design is system modeling. The limitations of modeling techniques lead to modeling uncertainties. Control systems become unpredictable and unstable as a result of these modeling uncertainties [5], [6]. These uncertainties have the potential to hinder the control performance. Modeling uncertainties can be divided into two categories: structured and unstructured [7], [8]. Unmodeled non-linearities lead to unstructured uncertainties, while unknown parameters of a known model lead to structured uncertainties

[8]. To address the aforementioned problems, researchers have developed disturbance observer (DOB) based control topologies [4], [9]. The DOB-based control topology proposed by Ohnishi differs from others; in the proposed DOB, user can modify the robustness of the system [9], [10]. There are two loops in this topology: an inner loop and an outer loop. The inner loop contains the DOB, which calculates the system's uncertainties and disturbances. A better robustness is then achieved by feeding back the estimated entities [9]. To meet the performance objectives, the outer loop is used while taking the nominal plant into account [6]. This can be accomplished using the RTOB tool if the nominal torque constant, nominal inertia, and nominal angular velocity are known beforehand.

By modifying the DOB to estimate the external torque/forces, Ohnishi et. al have developed the reaction torque observer (RTOB) [9], [11]. Compared to traditional force sensors, RTOB offers a number of benefits. In comparison to a conventional force sensor, it has a wider sensing bandwidth, which can be improved by reducing the sample time and raising the observer gain [11], [12]. The dynamics of the system are unaffected by the RTOB, however, as it is a virtual force sensor. The implementation of a force-senseless force controller has thus been made possible [11], [12].

Controlling how motion systems interact with their surroundings is a major issue in the industry [12]. Motion systems are subjected to unknown disturbances while carrying out tasks in an outside environment. In an uncertain environment, robust force tracking control is therefore necessary. The literature shows that the Ohinishi et al. have proposed two degree of freedom force control scheme is an exceptional choice to be used in uncertain environments [3], [12], [13].

The environment in contact is typically modeled as a spring and damper [9], [14]. Conventionally, the spring and damper are assumed to have constant coefficients throughout the motion when tuning the force controller. However, Harsha et al. have shown that the properties of the environment in contact exhibit a dynamic and nonlinear nature when motion parameters are altered [14]. Consequently, in some applications, the traditional approach to control system design is vulnerable.

This paper investigates the potential unstable scenarios of RTOB-based motion systems under the dynamic parameter variations in the environment in contact. In order to achieve

greater stability, it also proposes a technique for selecting the controller parameters that are particular to an application. In the final section, it is discussed how important is the system inertia is to the stability of the system.

The rest of the paper is organized as follows. The RTOB-based force controller integrated with the DOB is described in section II. The stability conditions for a continuous force controller model are deduced in section III's first subsection. The Routh Hurwitz criterion is used to analyze a transfer function for the RTOB output. The final section of section III examined the derived conditions with various environmental coefficients. In section IV, the results are explained. Conclusion and the design guidelines are presented in section V.

## II. DOB AND RTOB

### A. Disturbance Observer (DOB)

Figure 1 depicts a DC motor model with a DOB integrated. An estimation of externally uncertain disturbances like friction, inertia variation, and external loads are estimated by the DOB model's output.

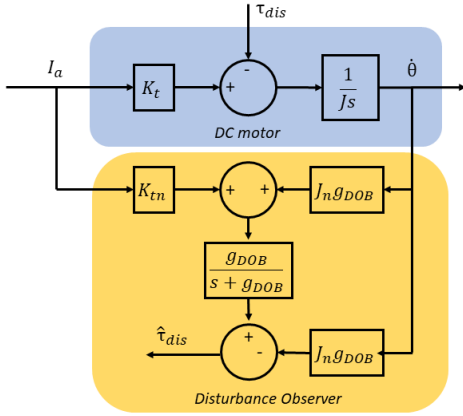


Fig. 1: A DC motor model integrated with a disturbance observer

The nominal torque constant and the nominal inertia are represented by  $K_{tn}$  and  $J_n$ , respectively. In reality, these values should either be pre-estimated or taken directly from the data provided by the manufacturer. The low pass filter's cutoff frequency is represented by  $g_{DOB}$ . Table I lists additional symbols and their typical representations.

The dynamic equation of the DOB model is found in equation (1)

$$\hat{\tau}_{dis} = (K_{tn}I_a + J_n g_{DOB} \dot{\theta}) \frac{g_{DOB}}{s + g_{DOB}} - J_n g_{DOB} \dot{\theta} \quad (1)$$

The estimated disturbance ( $\hat{\tau}_{dis}$ ) is defined in equation (2) as the sum of the frictional torques, external loads, and parameter uncertainties.

$$\hat{\tau}_{dis} = F_s + B\dot{\theta} + \tau_{int} + \Delta J_n \ddot{\theta} - \Delta K_{tn} I_a \quad (2)$$

TABLE I: Nomenclature

Parameter	Description	Value
$J_n/J$	Nominal/ Actual Inertia of the motor	0.00072 Nm
$K_{tn}/K_t$	Nominal/ Actual torque constant	0.135 NmA <sup>-1</sup>
$K_p$	Controller gain	
$\tau_{dis}/\hat{\tau}_{dis}$	Actual/ Estimated disturbance torque	
$\hat{\tau}_{ext}$	Estimated external torque	
$F_s$	Static friction of the motor	
$B$	Absolute Viscous friction coefficient	0.01 Nms/rad
$B_m$	Motor Viscous friction coefficient	0.01 Nms/rad
$K_{env}$	Stiffness of the environment in contact	10 Nm/rad
$\hat{\theta}$	Rotating velocity of the motor	
$g_{DOB}/g_d$	Cut off frequency value in DOB	300 s <sup>-1</sup>
$g_{RTOB}/g_r$	Cut off frequency value in RTDOB	300 s <sup>-1</sup>
$I_a$	Armature current of the motor	

### B. Reaction Torque Observer (RTOB)

The external impedances are estimated using a RTOB, which is depicted in figure 2. The RTOB model is a modified DOB which eliminates the effects of parameter variations and the frictional effects. In a system with one degree of freedom, the interactive torque, denoted by the parameters  $\tau_{int}$ , is zero, and the parameters  $g_{RTOB}$  denote the cutoff frequency of the RTOB. Despite the nearly identical control structures shown in figures 1 and 2, the latter is a model-based approach.

## III. ANALYSIS

### A. RTOB Integrated Enhanced Force Controller

Figure 3 depicts the force controller that is integrated with DOB and RTOB.  $K_p$  represents the controller gain. The nominal inertia/nominal torque constant factor is multiplied by the amplified force error to convert it to the current domain. To increase the robustness of the controller, the output of the disturbance observer is fed back into the system after being divided by the nominal torque constant in the inner loop. A spring damper is used to simulate the environment where the disturbance torque is applied.

Equation (4) is derived from figure 3 to represent the transfer function between the force command and the reaction torque observer estimation.

$$\frac{\hat{\tau}_{ext}}{\tau_{cmd}} = \frac{as^2 + bs + c}{As^4 + Bs^3 + Cs^2 + Ds + E} \quad (4)$$

$$\begin{aligned} a &= Bg_{RTOB}JK_p \\ b &= g_{RTOB}JK_p(Bg_{DOB} + K_{env}) \\ c &= g_{DOB}g_{RTOB}JK_{env}K_p \\ A &= J \\ B &= B + g_{DOB}J + g_{RTOB}J \\ C &= Bg_{RTOB} + g_{DOB}g_{RTOB}J + K_{env} + Bg_{RTOB}JK_p \\ D &= g_{RTOB}K_{env} + Bg_{DOB}g_{RTOB}JK_p + g_{RTOB}JK_{env}K_p \\ E &= g_{DOB}g_{RTOB}JK_{env}K_p \end{aligned}$$

$$f_1 = \frac{(B + g_{DOB}J)(Bg_{RTOB} + g_{RTOB}(g_{DOB} + g_{RTOB})J + K_{env}) + g_{RTOB}J(B^2 + Bg_{RTOB}J - JK_{env})K_p}{B + g_{DOB}J + g_{RTOB}J} > 0 \quad (3)$$

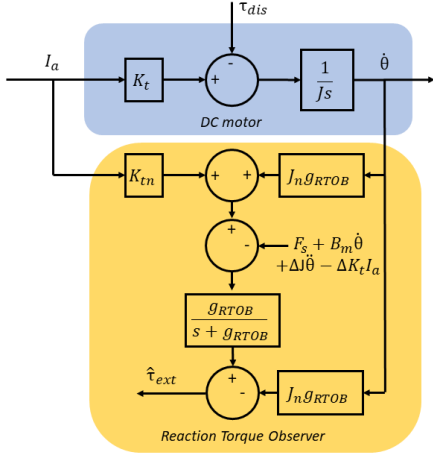


Fig. 2: A DC motor model integrated with a RTOB

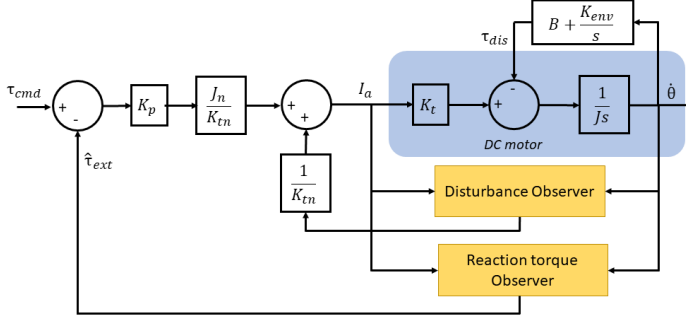


Fig. 3: A DC motor integrated force controller

### B. Study of Stability

Stability is studied using the characteristic equation displayed in equation (5).

$$As^4 + Bs^2 + Cs^2 + Ds + E = 0 \quad (5)$$

The derived characteristic equation is then subjected to Routh Hurwitz criterion and derived a conditions as in equation (3). Stability can be defined as a function of six variables using the derived equation. They can be divided into three categories: environmental variables, mechanical variables, and controller variables. Motor inertia  $J$  is classified as a mechanical variable, while the controller gain  $K_p$ , the cut off frequencies of the DOB and the RTOB,  $g_{DOB}$ , and  $g_{RTOB}$ , can be listed under controller variables.  $K_{env}$  and  $B_{env}$  can be categorized for the environmental variables because the environment in contact is modeled as a spring damper.

Environmental variables can be classified as uncertain variables because they frequently change with dynamic conditions like temperature and environment contraction, among other things. In order to remove environmental variables from the equation, the study was conducted assuming four different

environments as soft, neither soft nor hard, hard, and hardest.

TABLE II: Environment constant values used in simulations

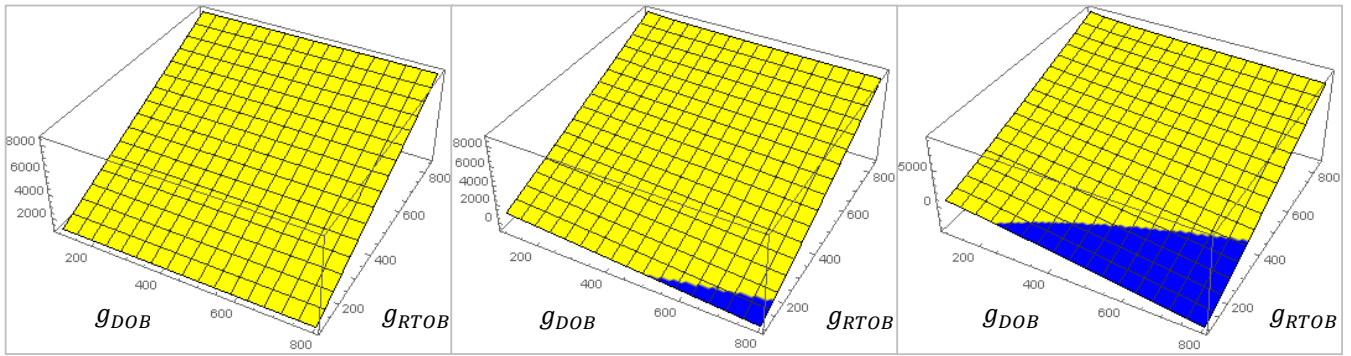
Environment nature	$K_{env}$	$B$
Soft	10 Nm/rad	0.01 Nms/rad
Neither hard or soft	100 Nm/rad	0.01 Nms/rad
Hard environment	1000 Nm/rad	0.01 Nms/rad
Hardest environment	1000 Nm/rad	0.1 Nms/rad

## IV. SIMULATION

By adjusting the controller and mechanical parameters, the stability conditions that were derived were visualized in three dimensions. The simulations for the soft environment are shown as graphs in figure 4. The effect of controller gain variation is depicted going from left to right. By assuming that the system has a higher inertia, the second row of the figure is obtained. The three other environmental models underwent the same set of simulations, which are shown in figures 5, 6 and 7. The  $g_{RTOB}$  and  $g_{DOB}$  values in a given graph are represented by the horizontal axes. The value of the function  $f_1$  is represented on the vertical axis. Stable and unstable regions were distinguished using two different color schemes. The possible dynamic parameter combinations that could stabilize the system are shown as yellow regions. The unstable combinations are displayed in the blue region. Table II lists the environmental constants used in the simulation.

The time domain analysis that was carried out to verify the stability analysis is shown in Figure 8. By adjusting the controller gain, Figure 8a is produced. The time domain analysis's mechanical and controller parameters are displayed in table I. The instability that develops when the inertia fluctuates while the other variables remain constant is depicted in Figure 8b. Figure 8c illustrates how stiffness of the environment affects stability. A situation where a system is stabilized by altering the cutoff frequency values independently while maintaining the other parameters constant is depicted in Figure 9.

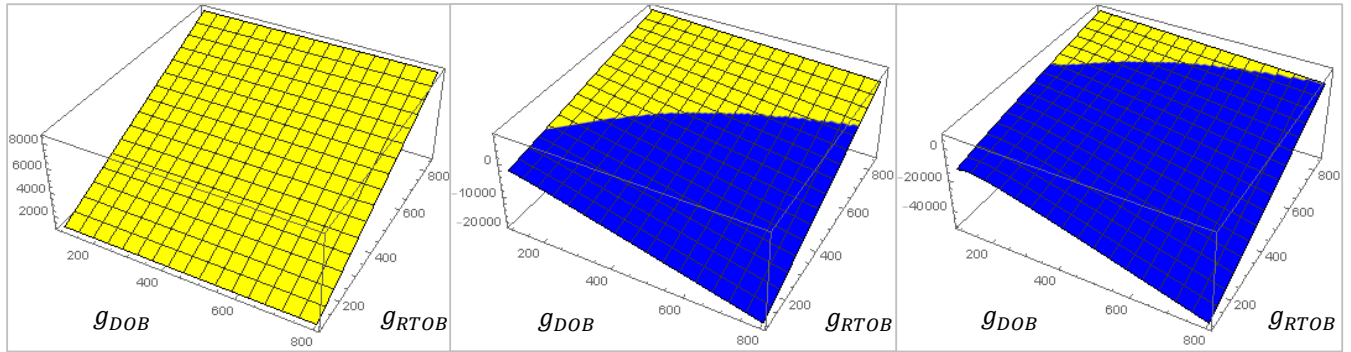
As the controller gain rises, it can be seen from figures 4, 5 and 6 that the stability zones get smaller. The controller gain effect is confirmed by the time domain response as depicted in Figure 8a. It has been demonstrated that the experiments performed at higher inertial values are highly unstable. This issue has been addressed by suggesting the use of lower controller gains. Force tracking performance, however, will be poor. In accordance with the analysis shown in Figures 5, 6 and 7, the stability is also attained by independently adjusting the cutoff frequencies while maintaining the other parameters at the desired values.



(a)  $J = 0.00072, P = 0.1$

(b)  $J = 0.00072, P = 400$

(c)  $J = 0.00072, P = 1000$

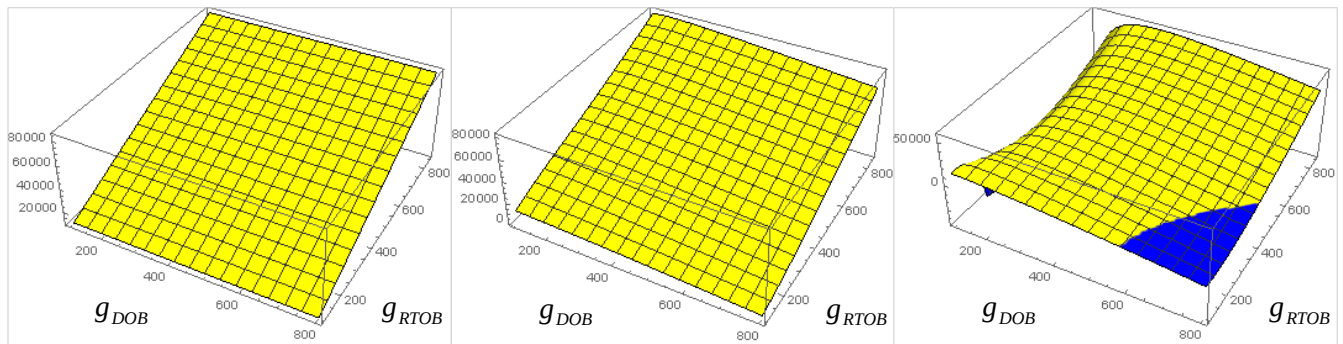


(d)  $J = 0.0072, P = 0.1$

(e)  $J = 0.0072, P = 400$

(f)  $J = 0.0072, P = 1000$

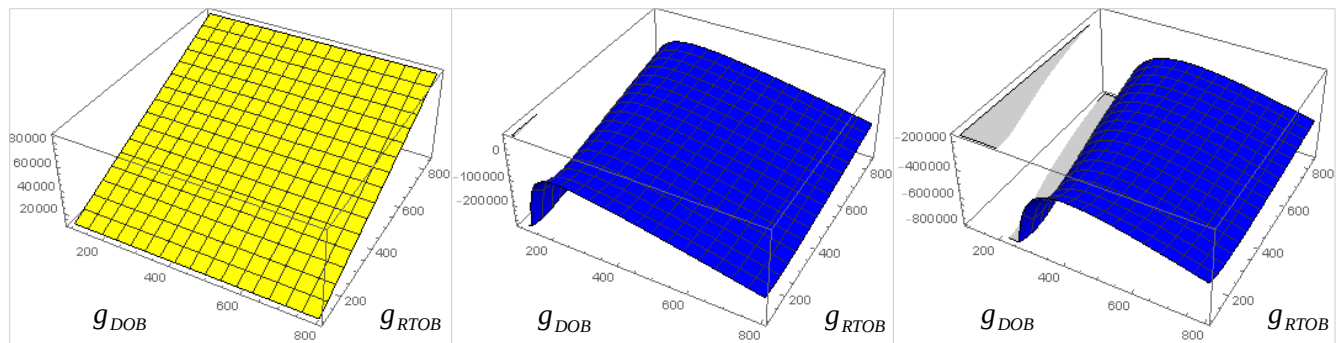
Fig. 4: Observation of Stability Variation under Soft Environment Conditions



(a)  $J = 0.00072, P = 0.1$

(b)  $J = 0.00072, P = 400$

(c)  $J = 0.00072, P = 1000$

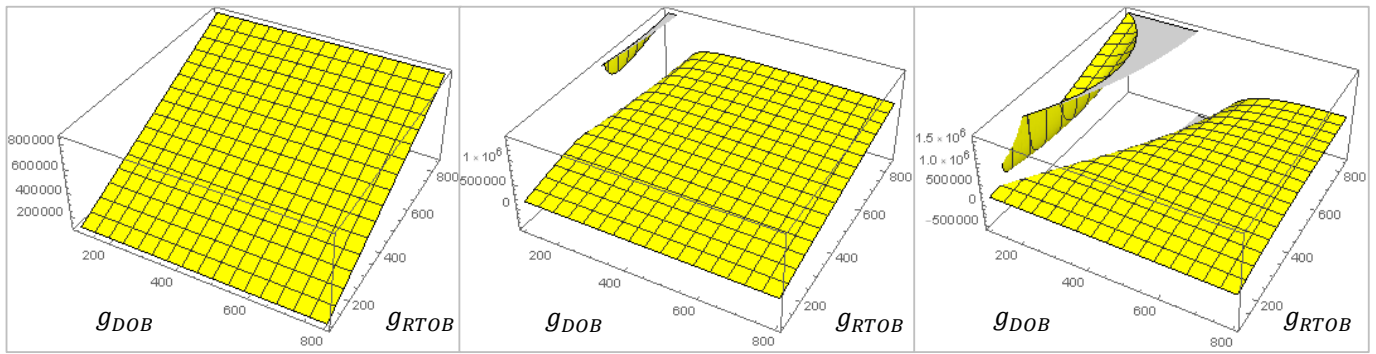


(d)  $J = 0.0072, P = 0.1$

(e)  $J = 0.0072, P = 400$

(f)  $J = 0.0072, P = 1000$

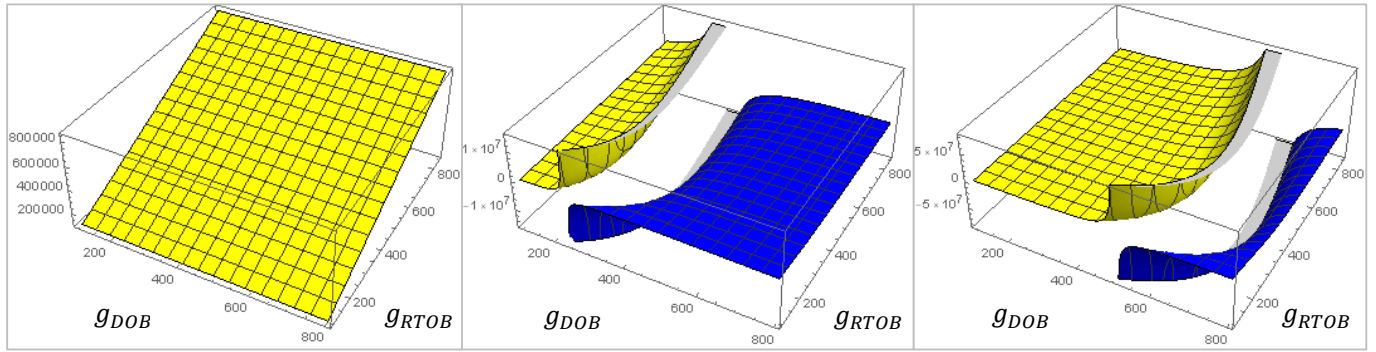
Fig. 5: Observation of Stability Variation under neither hard or Soft Environment conditions



(a)  $J = 0.00072, P = 0.1$

(b)  $J = 0.00072, P = 400$

(c)  $J = 0.00072, P = 1000$

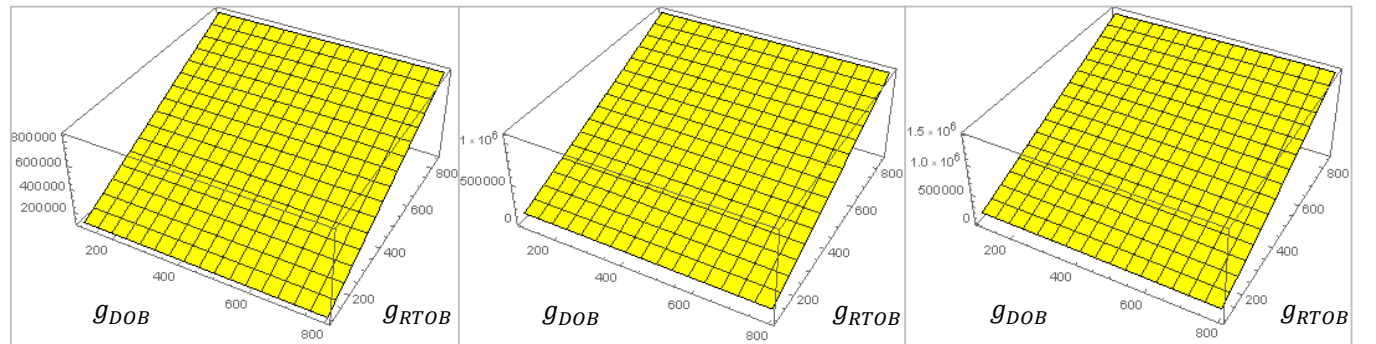


(d)  $J = 0.0072, P = 0.1$

(e)  $J = 0.0072, P = 400$

(f)  $J = 0.0072, P = 1000$

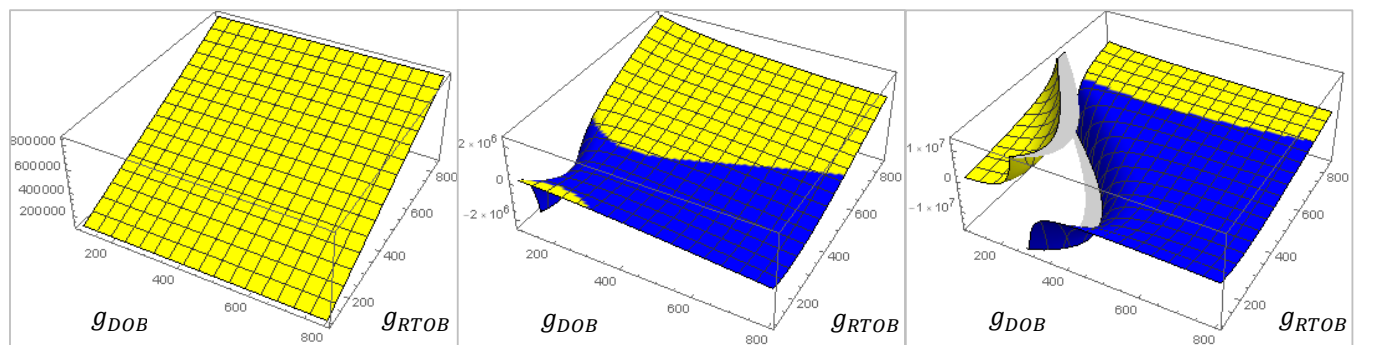
Fig. 6: Observation of Stability Variation under Hard Environment conditions



(a)  $J = 0.00072, P = 0.1$

(b)  $J = 0.00072, P = 400$

(c)  $J = 0.00072, P = 1000$



(d)  $J = 0.0072, P = 0.1$

(e)  $J = 0.0072, P = 400$

(f)  $J = 0.0072, P = 1000$

Fig. 7: Observation of Stability Variation under Hardest Environment conditions

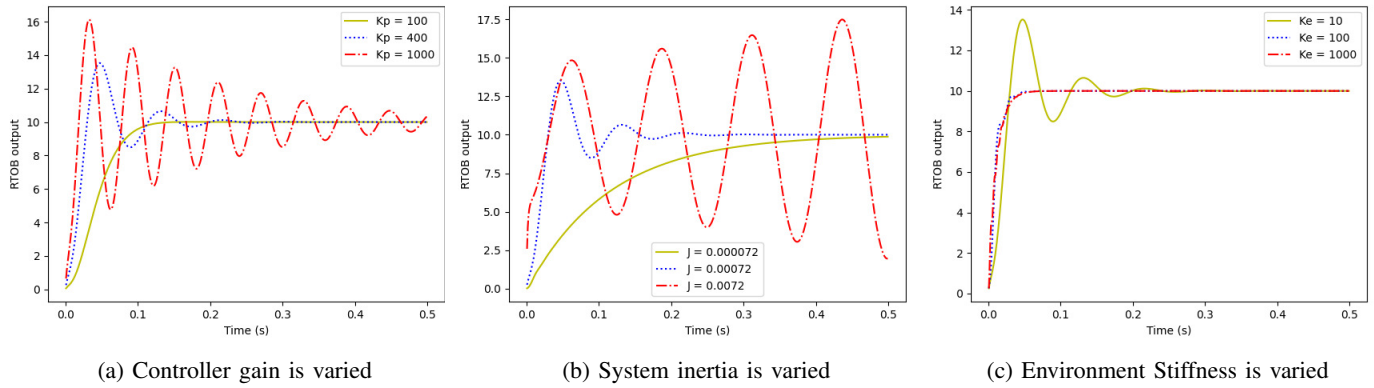


Fig. 8: Time Domain performance analysis against dynamic parameter variations

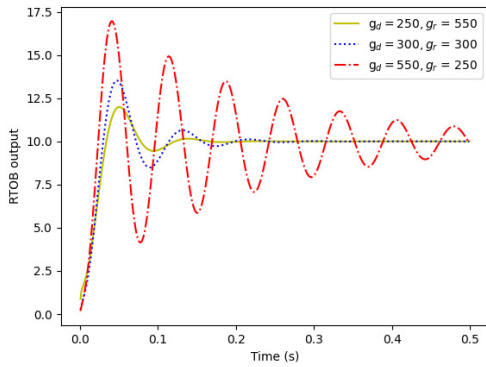


Fig. 9: RTOB stabilization by changing  $g_{DOB}$  and  $g_{RTOB}$  separately.

## V. CONCLUSION

This study investigates the conditions that lead to the instability of a force controller based on RTOB. It is demonstrated that the stability depends on mechanical, environmental, and controller dynamics. For force controller systems based on RTOB, a novel approach to stability assessment has been presented. The contact environment is assumed to be a spring damper, from which a transfer function is derived. The Routh-Hurwitz stability criterion was then used to analyze the derived equation. Different environmental, mechanical, and controller parameters were used to analyze a condensed but accurate stability condition.

Inertia  $J$ , a mechanical parameter, has been crucial in maintaining the stability. Force controllers based on RTOB are frequently unstable at higher inertial values. The controller gain can be reduced to stabilize the system. However, the force tracking performance will deteriorate. This paper analyzes and validates an effective method for doing this by tuning the two cutoff frequencies separately so that  $g_{DOB}$  is less than  $g_{RTOB}$ . Stability is significantly dependent on the environment. The controller should be tuned such that it satisfies  $g_{DOB} \ll g_{RTOB}$  if the environment in contact exhibits a lower stiffness. However, the best course of action is to keep  $g_{DOB} \approx g_{RTOB}$  if the environment exhibits a higher degree of stiffness. Viscosity typically has an impact on the stability, which is a parameter that can not be altered by the designer. The findings presented in this paper unequivocally

demonstrate the necessity of using the right parameter combinations when creating a force controller that employs DOB and RTOB.

## REFERENCES

- [1] S. Katsura, Y. Matsumoto, and K. Ohnishi, "Modeling of force sensing and validation of disturbance observer for force control," *IEEE Transactions on industrial electronics*, vol. 54, no. 1, pp. 530–538, 2007.
- [2] Y. Ohba, M. Sazawa, K. Ohishi, T. Asai, K. Majima, Y. Yoshizawa, and K. Kageyama, "Sensorless force control for injection molding machine using reaction torque observer considering torsion phenomenon," *IEEE Transactions on Industrial Electronics*, vol. 56, no. 8, pp. 2955–2960, 2009.
- [3] A. H. S. Abeykoon, W. Wijewardhana, E. H. Senevirathne, and K. Jayawardhana, "Vibration suppression of force controllers using disturbance observers," in *Vibration Control and Actuation of Large-Scale Systems*. Elsevier, 2020, pp. 57–89.
- [4] E. Sariyildiz, R. Oboe, and K. Ohnishi, "Disturbance observer-based robust control and its applications: 35th anniversary overview," *IEEE Transactions on Industrial Electronics*, vol. 67, no. 3, pp. 2042–2053, 2019.
- [5] W. T. G. Wijewardhana, E. H. Senevirathne, and A. H. S. Abeykoon, "Iterative approach for parameter estimation in dc motor based motion systems," in *2020 IEEE 29th International Symposium on Industrial Electronics (ISIE)*. IEEE, 2020, pp. 134–141.
- [6] E. Sariyildiz and K. Ohnishi, "Analysis of the robustness of control systems based on disturbance observer," *International Journal of Control*, vol. 86, no. 10, pp. 1733–1743, 2013.
- [7] J. Yao, Z. Jiao, and D. Ma, "Adaptive robust control of dc motors with extended state observer," *IEEE transactions on industrial electronics*, vol. 61, no. 7, pp. 3630–3637, 2013.
- [8] W. Sun, Z. Zhao, and H. Gao, "Saturated adaptive robust control for active suspension systems," *IEEE Transactions on industrial electronics*, vol. 60, no. 9, pp. 3889–3896, 2012.
- [9] E. Sariyildiz and K. Ohnishi, "Stability and robustness of disturbance-observer-based motion control systems," *IEEE Transactions on Industrial Electronics*, vol. 62, no. 1, pp. 414–422, 2014.
- [10] K. Ohnishi, M. Shibata, and T. Murakami, "Motion control for advanced mechatronics," *IEEE/ASME transactions on mechatronics*, vol. 1, no. 1, pp. 56–67, 1996.
- [11] H. Kobayashi, S. Katsura, and K. Ohnishi, "An analysis of parameter variations of disturbance observer for motion control," *IEEE Transactions on Industrial Electronics*, vol. 54, no. 6, pp. 3413–3421, 2007.
- [12] S. Katsura, Y. Matsumoto, and K. Ohnishi, "Analysis and experimental validation of force bandwidth for force control," *IEEE Transactions on Industrial Electronics*, vol. 53, no. 3, pp. 922–928, 2006.
- [13] E. Sariyildiz and K. Ohnishi, "Adaptive reaction torque/force observer design ii," in *2014 IEEE 23rd International Symposium on Industrial Electronics (ISIE)*. IEEE, 2014, pp. 1168–1173.
- [14] R. Ruwanthika and A. H. S. Abeykoon, "3d environmental force: Position impedance variation for different motion parameters," in *2015 Moratuwa Engineering Research Conference (MERCOn)*. IEEE, 2015, pp. 112–117.